

Figure 1. The absorption spectrum of the one-to-one complex between the truncated zinc finger peptide CP1-C4 and cobalt(II) in 50 mM HEPES, 50 mM NaCl buffer, pH 7.0. This spectrum is similar to that for complexes of intact zinc finger peptides although it is slightly broader and somewhat red-shifted due to the replacement of one histidine by a coordinated water. The schematic structure shown is supported by nuclear magnetic resonance studies of the parent CP1-Zn²⁺ complex.⁴ This and all other experiments were performed under an atmosphere of 95% dinitrogen/5% dihydrogen.

C4-Co²⁺ complex in the range $5 \times 10^{-8} - 2 \times 10^{-7}$ M. These values are less than 1 order of magnitude greater than that for the untruncated CP1-Co²⁺ complex. The stability of this complex was foreshadowed by the discovery of a low-pH form of the CP1-Zn²⁺ complex that has the latter of the histidines protonated and dissociated from the metal.⁵

The existence of an available coordination site on CP1-C4-Co²⁺ has been demonstrated by the availability of this complex to bind externally provided ligands. Titration of a solution of the peptide-Co²⁺ complex with β -mercaptoethanol resulted in series of spectra with isosbestic points as shown in Figure 2. The final spectrum is very similar to that obtained for the Co²⁺ complex of a sequence variant of CP1 in which the final histidine has been replaced with cysteine⁴ (also shown in Figure 2), providing strong support for the assignment of a three-thiolate, one-imidazole coordination sphere. A dissociation constant of 2×10^{-4} M at pH 8.0 was obtained from the titration data. Other ligands will also bind to CP1-C4-Co²⁺. Titration with *N*-methylimidazole produced a complex that has a spectrum nearly identical with that for the parent CP1-Co²⁺ complex that forms with a dissociation constant of 8×10^{-4} M at pH 8.0. Chloride will also bind although it does so rather weakly. Titration of an initially chloride free sample of the peptide-Co²⁺ complex with NaCl resulted in development of a somewhat red-shifted spectrum. The spectral changes could be fit with a dissociation constant of 0.8 M for chloride. Proof that chloride binding is weak is important since the other studies had been performed in the presence of ca. 50 mM Cl⁻ as part of the buffer solutions used. Control experiments with intact CP1 revealed no spectral changes with these ligands.

Thus, the truncation strategy has allowed the generation of a novel metallopeptide that has a coordination site available for the binding of externally added ligands. This site appears to be occupied by water in the absence of added ligands on the basis of the absence of any pH dependence of the spectrum up to pH 9 and consistent with the expected high pK_a for water bound to such a thiolate-rich site.⁷ The site is quite similar to the catalytic site in liver alcohol dehydrogenase,⁸ which is also capable of

(6) Metal ion titrations revealed the presence of a two peptide to one cobalt(II) complex that formed under conditions of high peptide-to-metal ratios. Deconvolution techniques allowed determination of the equilibrium constants for the formation of this species as well as the one-to-one complex. These results will be described in more detail in a subsequent publication (Schmidt, M. H.; Krizek, B. A.; Berg, J. M., manuscript in preparation).

(7) Bertini, I.; Luchinat, C.; Rosi, M.; Sgamellotti, A.; Tarentelli, F. *Inorg. Chem.* 1990, 29, 1460.

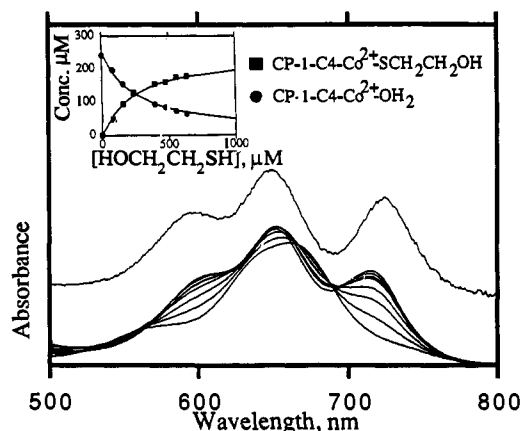


Figure 2. Titration of the cobalt(II) complex of CP1-C4 with β -mercaptoethanol. The absorption spectra upon addition of various amounts of β -mercaptoethanol are shown. The offset curves is from the cobalt(II) complex of the CP1 sequence variant in which the final histidine was replaced by cysteine.⁵ This spectrum is very similar to the CP1-C4-Co²⁺ spectra in the presence of saturating β -mercaptoethanol. The inset shows the experimental data from spectral deconvolution and the fit using a β -mercaptoethanol dissociation constant of 2×10^{-4} M. These experiments were performed in 50 mM HEPES, 50 mM NaCl, pH 8.0 buffer.

binding exogenous ligands. Initial attempts to demonstrate catalysis of reactions such as acetaldehyde hydration and *p*-nitrophenylacetate hydrolysis of Co²⁺ or Zn²⁺ complexes of CP1-C4 have not been successful. This lack of reactivity may be due to the apparent high pK_a of the coordinated water. Clearly more sophisticated design of a coordinatively unsaturated metal-based catalytic site will be required. Studies with other reactions and attempts to modify the properties of the peptide-metal complexes are in progress.

Acknowledgment. We thank the Office of Naval Research, The Chicago Community Trust/Searle Scholars Program, The Alfred P. Sloan Foundation, The National Science Foundation, Eli Lilly and Company, and E. I. du Pont de Nemours and Company for support of this work.

(8) Pettersson, G. In *Zinc Enzymes*; Bertini, I., Luchinat, C., Maret, W., Zeppezauer, M., Eds.; Birkhauser: Boston, MA, 1986.

Effect of Chain Length on the Energy Gap in Radical Ions of Oligomeric *p*-Phenylene¹

Rajive K. Khanna,* Yong M. Jiang, and David Creed

Department of Chemistry and Biochemistry
University of Southern Mississippi
Hattiesburg, Mississippi 39406

Received March 26, 1991

Revised Manuscript Received May 3, 1991

A dramatic increase in conductivity in poly(*p*-phenylene) (PPP), polythiophene, polypyrrole and other polyaromatics, upon oxidation or reduction (doping), is associated with the formation of charged defects (radical ions, diions)^{2,3} in the polymer matrix. Theoretical models⁴ predict the formation of radical ions (polarons) at low

(1) Khanna, R. K.; Jiang, Y. M. Presented in part at the symposium on Ion and Electron Conduction in Polymers, ACS combined Southeast-Southwest Regional Conference, New Orleans, LA, Dec 5-7, 1990; paper 19.

(2) Bredas, J. L.; Street, G. B. *Acc. Chem. Res.* 1985, 18, 309.

(3) (a) Patil, A. O.; Heeger, A. J.; Wudl, F. *Chem. Rev.* 1988, 88, 183.

(b) Frommer, J. E.; Chance, R. R. *Electrically Conductive Polymers*; In *Electrical and Electronic properties of Polymers*; Kroschwitz, J. I., Ed.; John Wiley & Sons: New York, 1988.

(4) (a) Bredas, J. L.; Chance, R. R.; Silbey, R. *Phys. Rev. B* 1982, 26, 5843. (b) Chung, T.-C.; Kaufman, J. H.; Heeger, A. J.; Wudl, F. *Phys. Rev. B* 1984, 30, 702.

Table I. Energy Gaps in Radical Ions of *p*-Phenylenes^a

radical ion (<i>n</i>) ^c	energy gaps, ^b eV	
	ΔE_1	ΔE_2
B ^{•+} (1)	2.6	
BP ^{•+} (2)	1.86	3.3
BP ^{•-} Li ⁺ (2) ^d	1.96	3.1
TP ^{•+} (3)	<1.4 ^e	2.96, 2.7
TP ^{•-} Li ⁺ (3) ^d	1.4	2.8, 2.6
QP ^{•+} (4)	<1.4 ^e	2.6
QP ^{•-} Li ⁺ (4)	1.05	2.6, 2.4
SP ^{•-} K ⁺ (6)	0.9	2.4, 2.2
SP ^{•-} Li ⁺ (6)	0.81	2.3
<i>p</i> -doped PPP (16) ^f	0.9	2.2

^aRadical cations are generated by laser flash photolysis of solutions of polyphenyls and ceric ammonium nitrate in MeCN at 351 nm. Radical anions are generated by reduction of the hydrocarbons with alkali metals in THF. ^bCalculated from observed electronic transitions in radical ions. ^cB = benzene; BP = biphenyl; TP = *p*-terphenyl; QP = *p*-quaterphenyl; SP = *p*-sexiphenyl; PPP = poly(*p*-phenylene); *n* = number of phenyl units in the oligomer. ^dValues from ref 17. ^eAbsorption extends beyond the spectral range of the monitoring system. ^fValues from ref 22.

oxidant/reductant concentrations, resulting in a narrowing of the energy gap between the highest bonding molecular orbital (HBMO) and the lowest antibonding molecular orbital (LABMO)²⁻⁵ of these conjugated macromolecules. This energy gap should also be dependent on the chain length of the polymer. We here report the first systematic investigation of the effect of chain length on HBMO-LABMO energy gap in radical ions of oligomeric *p*-phenylene. This has been accomplished by measuring the absorption spectra of radical cations, generated by a simple laser flash photolysis (LFP) method using ceric ammonium nitrate (CAN) as a photochemical oxidant, and radical anions of oligomers of PPP in acetonitrile (MeCN) and tetrahydrofuran (THF), respectively.

Excimer laser excitation (351 nm) of CAN in dry, deaerated MeCN yields^{6,7} the highly oxidizing⁸ nitrate radical, NO₃[•] (λ_{\max} at 602, 640, and 675 nm) which, in our hands, decays with first-order kinetics⁷ and a decay constant of $3.5 \times 10^5 \text{ s}^{-1}$. We find that in the presence of an oxidizable substrate⁹ the decay of NO₃[•] is accelerated¹⁰ with concomitant appearance of absorption attributed to the radical cation of the substrate. The electronic transitions¹¹ observed in the radical cations¹² thus generated from benzene (B^{•+}), biphenyl (BP^{•+}), *p*-terphenyl (TP^{•+}), and *p*-quaterphenyl (QP^{•+}) are listed in Table I. None of the substrate hydrocarbons absorb substantially at 351 nm, and thus they do not yield any transients in the absence of CAN. Since the spectra of BP^{•+} and TP^{•+} obtained by radiolytic methods¹³ in CCl₄ glass are very similar to those obtained by us in MeCN,¹⁴ we presume

that ion-pairing of radical cations in MeCN solvent is negligible. Thus, the CAN/LFP technique provides a simple and direct method for the generation and observation of radical cations of aromatic hydrocarbons. The NO₃[•] absorbs minimally^{8b} ($\epsilon_{635} \sim 1000 \text{ M}^{-1} \text{ cm}^{-1}$) and is thus better than SO₄^{•-} for these and similar studies.¹⁵

Radical anions of polyphenyls were generated by reduction of the oligomers with alkali metals¹⁶ at 30 °C in deaerated THF. They display absorption characteristics (Table I) similar to those of the corresponding radical cations, which is in accord with earlier observations^{17,18} on radical ions of even-alternant hydrocarbons. These radical anions do not decay appreciably on the time scale (1–2 h) of our experiment.

Undoped poly(*p*-phenylene) is characterized by an energy gap of 3.6 eV associated with an interband transition derived from the π - π^* transition of the phenylene moiety.¹⁹ The corresponding energy gaps^{20,21} for benzene, biphenyl, *p*-terphenyl, *p*-quaterphenyl, and *p*-sexiphenyl are 5.9, 4.92, 4.43, 4.15, and 3.9 eV, respectively. Although the absorption maxima shift into the visible, when the chain length is increased, PPP remains an insulator without doping. One-electron oxidation (*p*-doping) or reduction (*n*-doping) of these even-alternant aromatic hydrocarbons results in the appearance of two doping-induced energy levels, bonding and antibonding, which are symmetric with respect to the gap center.²⁻⁴ Thus the energy gap between the HBMO and the LABMO narrows, as is evident from the values for low-energy transitions (ΔE_1) listed in Table I. The high-energy transitions (ΔE_2) may be attributed to collective excitations of the lower level degenerate π electrons (valence band) to the LABMO and to similar energy HBMO to conduction band (higher degenerate antibonding levels) transitions. It is interesting to note that *p*-doped PPP displays similar transitions²² at ca. 0.9 and 2.2 eV.

A correlation of the HBMO-LABMO energy gap (ΔE_1) in radical ions of oligomeric *p*-phenylene with chain length suggests that this energy gap decreases with an increase in the numbers of phenyl units (*n*) in the oligomer but reaches a limiting free carrier value for *n* ~ 6. It is intriguing to note that the conductivity in pressed pellets of *n*-doped polyphenyls initially increases dramatically with the chain length but reaches a limiting value for *p*-sexiphenyl.²¹ Although conductivities in pressed pellets may be limited by interparticle resistance,²¹ our results demonstrate an inverse relationship between conductivity and the HBMO-LABMO energy gap in doped polyphenyls, with a limiting value for both attained at *n* ~ 6. Since short chain length conjugated molecules are easier to process via solubilization and formation of composites, demonstration of high "intrinsic" conductivities in these materials may increase their potential for commercial applications.

(14) (a) It is interesting to note that pulse radiolysis of solutions of biphenyl in both CCl₄ and CHCl₃ gives a transient absorption spectrum with a maximum at approximately 550 nm, whereas in other halogenated solvents such as 1,2-dichloroethane and *n*-butyl chloride, a spectrum of BP^{•+}, similar to that obtained by us, is observed.^{14b} The band at 550 nm in CCl₄ may be attributed to a charge-transfer complex of biphenyl with chlorine atoms, which are known^{14c} to be generated in this solvent. It should be noted that the longer wavelength bands, attributed to the radical cations, in 1,2-dichloroethane show a small red shift (20 nm) compared to our observations in MeCN solvent. (b) Arai, S.; Ueda, H.; Firestone, R. F.; Dorfman, L. M. *J. Chem. Phys.* **1969**, *50*, 1072. (c) Chateaneuf, J. E. *J. Am. Chem. Soc.* **1990**, *112*, 442.

(15) McClelland, R. A.; Mathivanan, N.; Steenken, S. *J. Am. Chem. Soc.* **1990**, *112*, 4857.

(16) Electrical conductance measurements¹⁷ show that whereas lithium salts of aromatic radical anions in THF are completely dissociated at room temperature, potassium salts are ion-paired.

(17) Buschow, K. H. J.; Dielman, J.; Hoijtink, G. J. *J. Chem. Phys.* **1965**, *42*, 1993.

(18) Dorfman, L. M. *Acc. Chem. Res.* **1970**, *3*, 224.

(19) Su, Z.; Yu, L. *Phys. Rev. B* **1983**, *27*, 5199 and references cited therein.

(20) Bredas, J. L.; Silbey, R.; Boudreaux, D. S.; Chance, R. R. *J. Am. Chem. Soc.* **1983**, *105*, 6555.

(21) Shacklette, L. W.; Eckhardt, H.; Chance, R. R.; Miller, G. G.; Ivory, D. M.; Baughman, R. H. *J. Chem. Phys.* **1980**, *73*, 4098.

(22) (a) These have been assigned to transitions in the bipolaron^{22b} (diion), but in view of our results with other oligomers, they match the expected transitions in the polaron (radical ion) of PPP. (b) Creelius, G.; Stamm, M.; Fink, J.; Ritsko, J. *J. Phys. Rev. Lett.* **1983**, *50*, 1498.

(5) Schaffer, H. E.; Heeger, A. J. *Solid State Commun.* **1986**, *59*, 415.

(6) (a) Khanna, R. K.; Sutherland, J. S.; Lindsey, D. *J. Org. Chem.* **1990**, *55*, 6233. (b) Baciocchi, E.; Giacco, T. D.; Murgia, S. M.; Sebastiani, G. V. *J. Chem. Soc., Chem. Commun.* **1987**, 1246.

(7) Glass, R. W.; Martin, T. W. *J. Am. Chem. Soc.* **1970**, *92*, 5084.

(8) (a) Electron affinity of NO₃[•] is 3.7 eV.^{8b} (b) Akiho, S.; Ito, O.; Iino, M. *Int. J. Chem. Kinet.* **1989**, *21*, 667.

(9) In typical experiments, LFP of CAN (0.05–0.5 mM) in dry, deaerated MeCN in the presence of an aromatic hydrocarbon substrate (0.02–5.0 mM) yielded the absorption spectrum of the transient radical cation of the hydrocarbon, which was recorded 200 ns–2.0 μ s after the laser pulse. The initial concentration of NO₃[•] ($1.5 \times 10^{-6} \text{ M}$ – $1.5 \times 10^{-5} \text{ M}$), under these conditions, is lower than that of the substrate hydrocarbon.

(10) The pseudo-first-order rate constant for the formation of BP^{•+}, measured at 380 nm, is in excess of $1 \times 10^8 \text{ s}^{-1}$. Similar rate constants are obtained with other hydrocarbons.

(11) Absorption bands attributed to each radical cation decay with identical kinetics.

(12) (a) In our hands, the radical cations have lifetimes up to a few microseconds and their decay is mixed order.^{12b} Although the rates of decay are dependent on the concentration of CAN, under comparable conditions the lifetimes increase with increasing conjugation. (b) Parker V. D. *Acc. Chem. Res.* **1984**, *17*, 243.

(13) (a) Shida, T.; Hamill, W. H. *J. Chem. Phys.* **1966**, *44*, 2375. (b) Shida, T. *Electronic Absorption Spectra of Radical Ions*; Elsevier: Amsterdam, 1988.

Further studies with higher oligomers of *p*-phenylene and oligomers of pyrrole and thiophene are being pursued, as are further applications of the CAN/LFP technique for generation of radical cations.

Acknowledgment. Support of this research by the National Science Foundation EPSCoR program and the donors of the Petroleum Research Fund, administered by the American Chemical Society, is gratefully acknowledged. We thank Ms. Kezi Ezell and Mr. Troy Lewis for invaluable technical assistance.

Supplementary Material Available: Absorption spectra of transient NO_3^{\cdot} (550–700 nm), $\text{B}^{+\cdot}$ (400–520 nm), $\text{BP}^{+\cdot}$ (370–810 nm), $\text{TP}^{+\cdot}$ (400–550 nm), $\text{TP}^{+\cdot}$ (810–900 nm), $\text{QP}^{+\cdot}$ (400–550 nm), and $\text{QP}^{+\cdot}$ (710–900 nm) in MeCN solvent, absorption spectra of $\text{Li}^+\text{QP}^{\cdot-}$ (400–800 nm), $\text{Li}^+\text{QP}^{\cdot-}$ (12000–6000 cm^{-1}), $\text{Li}^+\text{SP}^{\cdot-}$ (400–800 nm), $\text{K}^+\text{SP}^{\cdot-}$ (350–900 nm), and $\text{Li}^+\text{SP}^{\cdot-}$ (12000–6000 cm^{-1}) in THF solvent, and a decay trace for NO_3^{\cdot} in MeCN solvent (13 pages). Ordering information is given on any current masthead page.

A Ru(II) Enynyl Complex Mediates the Catalytic Dimerization of 1-Alkynes to *Z*-1,4-Disubstituted Enynes

Claudio Bianchini,^{*,†} Maurizio Peruzzini,^{*,†}
Fabrizio Zanobini,[†] Piero Frediani,[‡] and Alberto Albinati[§]

*Istituto per lo Studio della Stereochimica ed
Energetica dei Composti di Coordinazione, CNR
Via J. Nardi 39, 50132, Firenze, Italy
Dipartimento di Chimica Organica
Università di Firenze, Firenze, Italy*

*Istituto Chimico
Farmaceutico e Tossicologico dell'Università di Milano
Milano, Italy*

Received February 27, 1991

Detailed mechanistic studies on metal-assisted dimerization reactions of 1-alkynes to butenyne¹ have not been published, and the factors that govern regio- and stereoselectivity are not yet fully understood.

Herein we report that the selective coupling of terminal alkynes to *Z*-1,4-disubstituted butenyne can be achieved in a catalytic way by using either the Ru(II) $\eta^2\text{-H}_2$ complex $[(\text{PP}_3)\text{Ru}(\text{H})(\text{H}_2)]\text{BPh}_4$ (1) or the η^1 -dinitrogen derivative $[(\text{PP}_3)\text{Ru}(\text{H})(\text{N}_2)]\text{BPh}_4$ (2) [$\text{PP}_3 = \text{P}(\text{CH}_2\text{CH}_2\text{PPh}_2)_3$].² We describe in detail the reaction sequence leading to 1,4-bis(trimethylsilyl)-but-3-en-1-yne, but comparisons with other 1-alkynes are given in the text showing the applicability of our method to the catalytic homo coupling and stoichiometric cross coupling of 1-alkynes.

When a solution of 2 (or 1) in THF is stirred for 1 h under argon or nitrogen with 3 (or 4) equiv of $\text{HC}\equiv\text{CSiMe}_3$, 1 (or 2) equiv of vinyltrimethylsilane and canary yellow crystals of (*E*)- $[(\text{PP}_3)\text{Ru}\{\eta^3\text{-(SiMe}_3)_3\text{C}_3\text{CH(SiMe}_3)\}]\text{BPh}_4$ (3) are obtained. The molecular structure of the complex cation of 3-acetone is

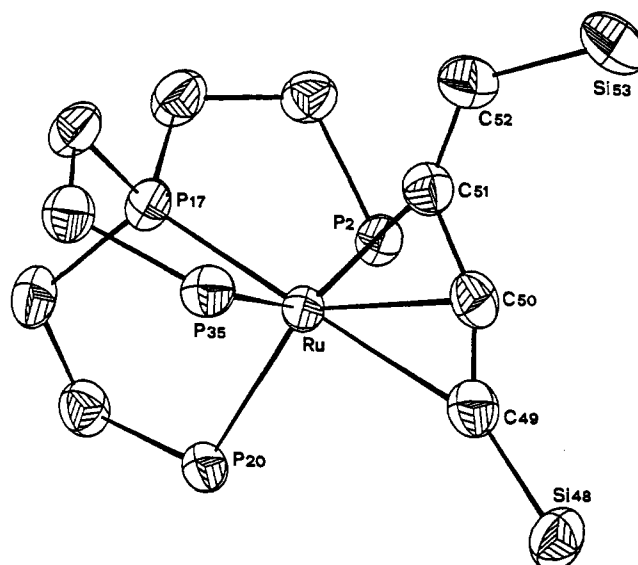


Figure 1. ORTEP drawing of the complex cation in 3. Phenyl rings are omitted for clarity. The relevant geometric features are as follows: Ru–P 2.342 (1) (av), Ru–C(49) 2.485 (3), Ru–C(50) 2.234 (3), Ru–C(51) 2.144 (3), C(49)–C(50) 1.247 (5), C(50)–C(51) 1.392 (5), C(51)–C(52) 1.335 (5) Å; P(2)–Ru–C(51) 81.57 (9), P(17)–Ru–C(49) 172.1 (1), P(17)–Ru–C(51) 107.9 (1), P(20)–Ru–C(51) 166.30 (9), P(35)–Ru–C(50) 89.17 (9), C(49)–C(50)–C(51) 154.0 (3), C(50)–C(51)–C(52) 133.5 (3), C(50)–C(49)–Si(48) 142.0 (3), C(51)–C(52)–Si(53) 126.0 (3)°.

shown in Figure 1.³ The coordination geometry around ruthenium is distorted octahedral with four coordination positions occupied by the phosphorus atoms of PP_3 and the remaining edge taken by the butenyne ligand. The bond distances between ruthenium and the atoms C(50) [$\text{C}\equiv\text{CSiMe}_3$] and C(51) [$\text{C}=\text{C}(\text{H})\text{SiMe}_3$] [2.234 (3) and 2.144 (3) Å, respectively] are in line with those found for other η^3 butenyne complexes.⁴ The weakest interaction is present with C(49) [CSiMe_3] [2.485 (2) Å] and probably originates from repulsion between the Si(48) SiMe_3 group and the many phenyl rings. The C–C bond distances within the η^3 -butenyne ligand are suggestive of some degree of electronic delocalization.

Monitoring the reactions between 2 and variable amounts of $\text{HC}\equiv\text{CSiMe}_3$ by $^3\text{P}\{^1\text{H}\}$ and ^1H NMR shows that the butenyne 3 forms by addition of 1 equiv of alkyne to the σ -alkynyl $[(\text{PP}_3)\text{Ru}(\sigma\text{-C}\equiv\text{CSiMe}_3)]\text{BPh}_4$ (4) isolable in the solid state as red crystals of the THF solvate. In turn, 4 quantitatively forms by reaction of $\text{HC}\equiv\text{CSiMe}_3$ with (*E*)- $[(\text{PP}_3)\text{Ru}\{\text{C}(\text{H})=\text{CH}(\text{SiMe}_3)\}]\text{BPh}_4$ (5), which is obtained by trans insertion [$J(\text{HH}) = 18.1$ Hz] of the alkyne across the Ru–H bond (Scheme 1). Pure samples of the σ -alkynyl complex 5 cannot be obtained since its reaction with the alkyne to give 4 is much faster than that of the alkyne with 2. As a matter of fact, treatment of 2 with 1 equiv of $\text{HC}\equiv\text{CSiMe}_3$ invariably yields mixtures of 2, 4, and 5. The result of the reaction of 2 with $\text{HC}\equiv\text{CSiMe}_3$ invariably yields mixtures of 2, 4, and 5. The result of the reaction of 2 with $\text{HC}\equiv\text{CCO}_2\text{Et}$ yielding (*G*)- $[(\text{PP}_3)\text{Ru}\{\text{C}(\text{COOEt})=\text{CH}_2\}]\text{BPh}_4$ (6) confirms that the insertion of the alkyne across the Ru–H bond is the first step.⁵ The geminal structure of the alkenyl ligand is in keeping with the electron-withdrawing character of the carboxy substituent.⁶

[†] Istituto ISSECC CNR.

[‡] Università di Firenze.

[§] Università di Milano.

(1) (a) Keim, W.; Behr, A.; Röper, M. In *Comprehensive Organometallic Chemistry*; Wilkinson, G., Stone, F. G. A., Abel, E. W., Eds.; Pergamon: New York, 1982; Vol. 8, p 371. (b) Trost, B. M.; Chan, C.; Ruhter, G. *J. Am. Chem. Soc.* 1987, 109, 3486. (c) Kovalek, I. P.; Yevdakov, K. V.; Strelenko, Y. A.; Vinogradov, M. G.; Nikishin, G. I. *J. Organomet. Chem.* 1990, 386, 139. (d) Ishikawa, M.; Ohshita, J.; Ito, Y.; Minato, A. *J. Organomet. Chem.* 1988, 346, C58.

(2) Bianchini, C.; Perez, P. J.; Peruzzini, M.; Zanobini, F.; Vacca, A. *Inorg. Chem.* 1991, 30, 279.

(3) Crystals suited for an X-ray analysis were obtained by recrystallization from acetone/ethanol: triclinic crystal, space group $P\bar{1}$, $a = 15.495$ (2) Å, $b = 15.596$ (2) Å, $c = 17.006$ (2) Å, $\alpha = 116.14$ (2)°, $\beta = 94.03$ (2)°, $\gamma = 97.38$ (2)°, $Z = 2$, $d_{\text{calcd}} = 1.233$ g cm^{-3} , $n_{\text{obsd}} = 7565$, $R = 0.0351$. A clathrated molecule of acetone was located in the cell.

(4) (a) Jia, G.; Rheingold, A. L.; Meek, D. W. *Organometallics* 1989, 8, 1378. (b) Gotzlig, J.; Otto, H.; Werner, H. *J. Organomet. Chem.* 1985, 287, 247.

(5) Lundquist, E. G.; Folting, K.; Streib, W. E.; Huffmann, J. C.; Eisenstein, O.; Caulton, K. G. *J. Am. Chem. Soc.* 1990, 112, 855.